

Copper tailings filtration: Influence of filter cake desaturation

Bernd Fränkle^{a,*}, Thien Sok^b, Marco Gleiß^a, Hermann Nirschl^a

^a Institute of Mechanical Process Engineering and Mechanics, Karlsruhe Institute of Technology, Karlsruhe, Germany

^b Salt Lake City Operations, FLSmidth Inc., Midvale, USA

ARTICLE INFO

Keywords:

Tailings
Filtration
Copper
Filter cake
Desaturation
Adhesion
Cohesion

ABSTRACT

Copper mining produces immense amounts of tailings due to low ore grades. These residues are increasingly dewatered by filtration in recessed plate filter presses to ensure safer storage and high recovery of water. The process parameters filtration pressure, desaturation time, desaturation pressure and cake thickness have a significant influence on achieving water content as well as bulk material stability specifications and maintaining operation performance, especially with regard to cake detachment. In this study, copper tailings filtration tests in a laboratory filter press and directly connected measurements of cake-to-fabric shear adhesion as well as filter cake shear cohesion were carried out. It is shown that optimization of cake properties with regard to residual water content, suitability for detachment and bulk material stability by specific adjustment of the filtration and post-treatment parameters is possible. Furthermore, implementation of a mathematical model allows water content, cake saturation, cake-to-fabric shear adhesion and cake shear strength prediction dependent on filter cake desaturation time and pressure for tailings filtration applications in recessed plate filter presses.

1. Introduction

Increasing growth of population, technological progress and change in the energy and mobility sectors cause a steady rise in demand for metallic and mineral commodities. Copper, lithium, cobalt and nickel, which are essential for electric vehicles, are just four of many examples (FLSmidth Minerals Technology Center, 2019). Ore mining, as the basis for the extraction of metals and minerals, is carried out in open-pit or underground operations. The mining cycle can be divided into exploration, evaluation, exploitation, mineral processing and reclamation (Bustillo Revuelta, 2017). The mineral processing step represents the concentration of the valuable metals or minerals in order to enable profitable transport and extraction (Wills and Finch, 2015). This is done by crushing, separation, for example by froth flotation, and solid-liquid separation (Concha, 2014). Since most of the processes in mineral engineering require a large amount of water, water management and recovery are important considerations (Bleiwas, 2012; Gunson et al., 2012).

Only a small portion of the mined rock is valuable mineral (Mortimer and Müller, 2007). A large amount of waste results from overburden, waste rock and ore residues. The latter are the milled but valueless part of the ore, also called tailings (Higman et al., 2019). Furthermore, these tailings come out of the process as a suspension containing most of the

process water (Jewell and Fourie, 2015). The traditional way to dispose this slurry in settling ponds causes a variety of problems such as enormous land footprint, water loss, dam failures and environmental contamination (Roche et al., 2017; Kossoff et al., 2014; Lottermoser, 2010; Lottermoser, 2017). The regularity of dam breaches (Islam and Murakami, 2021; Piciullo et al., 2022) and the increasing necessity to recover water led to the development of methods of disposing of tailings with less water, e.g. thickened or paste tailings, in the second half of 20th century (Jewell and Fourie, 2015). However, these actions can still be insufficient. More recent dam breaches and increased media attention reinforced the development and regulations were tightened and new standards established (Baker et al., 2020; International Council on Mining and Metals (ICMM), 2020). In addition to thickened or paste disposal, tailings are now increasingly being filtered and then stacked (Davies and Rice, 2001; Davies, , 2011). This enables safer storage, higher water recovery rates and further reduction of footprint (Morrill et al., 2022).

Due to the particle size distribution with a high proportion of fines (Wang et al., 2014) and the necessity to achieve sufficient dewatering and compacting, filter presses are used very often (Jewell and Fourie, 2015). According to ISO specifications in the geotechnical context a particle size of 63 μm is considered as fines (ISO, 2017). Despite the optimization in terms of capacity and throughput, several filter presses

* Corresponding author.

E-mail addresses: bernd.fraenkle@kit.edu (B. Fränkle), thien.sok@flsmidth.com (T. Sok), marco.gleiss@kit.edu (M. Gleiß), hermann.nirschl@kit.edu (H. Nirschl).

must be operated in parallel in a mine (Rahal and Wisdom, 2020). For an application with 100,000 tons per day, seven large filter presses, e.g. FLSmidth AFP 2040 with a filtration area up to 2040 m² and 38.4 m³ in one machine (FLSmidth Minerals Technology Center, 2012), are necessary (Jewell and Fourie, 2015). A target water content of 20 % can be assumed (Gomes et al., 2016). Thereby, tailings transportation on conveyor belts and stacking is possible, and, in general, a sufficient geotechnical stability and water recovery rate is reached. Especially achieving such water contents by desaturation of the filter cake using pressurized air desaturation inhibit liquefaction of the stack due to a high shear cohesion, which is also referred to as shear strength (Davies and Rice, 2001).

However, operation of tailings filtration plants is a challenging task. Besides cloth lifetime related issues like abrasive wear or blinding by adhering particles (Fränkle et al., 2022; Fränkle et al., 2023; Fränkle et al., 2021; Blanchet, 2018; Wisdom, 2019), achievement of the required target water content as well as predicting cycle time including filtration and technical time correctly is crucial. Both require a sufficient understanding of the filtration process in the filter press: For maximized throughput target water content has to be reached as fast as possible, e. g., by a short pressurized air cake post-treatment resulting in desaturation. Moreover, a good cake detachment is required for keeping technical downtime low. Detachment behavior depends mainly on cake-to-fabric adhesion and cake stability which is also referred to as cohesion. In general, cakes having a low cake-to-fabric shear adhesion and behaving more brittle, i.e., having a high shear cohesion, detach easier (Weigert, 2001).

Filter cake thickness, application time and air pressure are crucial parameters of the gas differential pressure desaturation post-treatment and influence the kinetics of the so-called air blow. An approach to describe the desaturation kinetics for incompressible filter cakes was given by Nicolaou, according to Eq. (1) (VDI, 2017; Nicolau, 1999). $S(t)$ describes the time-dependent saturation of the voids in the filter cake, S_∞ is the saturation value at equilibrium for a certain desaturation pressure Δp . Also, the capillary entry pressure p_{ce} , the thickness specific cake resistance α_n , the cake porosity ε , the dynamic viscosity of the liquid η_l , the cake thickness T and two fit parameters a and b are used.

$$\frac{S(t) - S_\infty}{1 - S_\infty} = \left(1 + a \cdot \frac{\Delta p - p_{ce}}{\alpha_n \cdot \varepsilon \cdot \eta_l \cdot T^2} \cdot t \right)^{-b} \quad (1)$$

The value of saturation at equilibrium for a certain gas differential pressure is a result of the capillary inlet pressure distribution and, thus, is given by the capillary pressure curve (Anlauf, 2019). Within the cake complete regions can have higher inlet pressures than the air blow pressure applied. This leads to isolated pores filled with water which limit the final water content that can be reached significantly (Anlauf, 2019). Since compaction depends on filtration pressure and saturation at equilibrium depends on air blow pressure, an increase in cake thickness alters the air-blow time, and hence overall cycle time and capacity (Anlauf, 2019). Thicker cakes need more desaturation time to reach equilibrium (Anlauf, 2019). After the post-treatment, the plate stack opens, the filter cakes detach and fall down.

The cake detachment process and the underlying mechanisms are very interdisciplinary. Previous publications and guidelines can be found in fields of filtration (Fränkle et al., 2022; Weigert and Ripperger, 1997; Ozcan et al., 2000; Fränkle et al., 2021), bulk material (Hammerich et al., 2020), geotechnical applications (Xiu et al., 2023) and rheology (Das et al., 2023) showing significant influences of compaction and desaturation on particulate network properties. These properties are mainly water content, saturation, cake-to-fabric adhesion and cohesion. Cohesion can be divided into tensile and shear cohesion both having a maximum of tensile and shear strength concerning level of saturation (Ozcan et al., 2001; Ozcan et al., 2000; Ozcan et al., 2000; Schubert, 1972; Rumpf, 1974; Schubert, 1982).

Key findings of literature review and a previous study of tailings lab-

scale filtration including adhesion and cohesion tests using iron ore tailings are (Fränkle et al., 2022; Weigert, 2001):

- Tailings are considered to generate slightly compressible filter cakes.
- The cake properties shear adhesion and shear cohesion are strongly dependent on process parameters, especially filtration pressure, desaturation time and desaturation pressure.
- Overcoming shear adhesion between filter cake and filter fabric by cake weight (mainly dependent on cake thickness) is crucial. The sealing edge influence increases the weight needed.
- Cake stability (cohesion) must be high enough for detachment.

The assumed main underlying mechanism for cake detachment in filter presses is that the gravitational force F_g of the cake overcomes the cake-to-fabric adhesion F_a . If cake stability is sufficient and influence of sealing edges and protruding parts is neglected, the force balance according to Eq. (2) describes cake detachment (Fränkle et al., 2022; Weigert, 2001; Fränkle et al., 2021). T_c is the thickness, W_c the width, H_c the height, ε the porosity and S the void saturation of the cake. ρ_s is the density of the solids and ρ_l the density of the fluid.

$$T_c \cdot W_c \cdot H_c \cdot ((1 - \varepsilon) \cdot \rho_s + \varepsilon \cdot S \cdot \rho_l) \cdot g = F_g > F_a \quad (2)$$

Measurement of cake-to-fabric adhesion can be used to calculate the necessary cake thickness to overcome the shear adhesion to initiate detachment (Weigert, 2001). However, the resulting cake thickness is often above typical chamber dimension for recessed plate filter presses of 30–60 mm (Fränkle et al., 2022; Outotec, 2022), where, nevertheless, detachment is observed (Fränkle et al., 2022). One reason is the simplification by the model. For example, Weigert stated that measured area-related adhesion values become smaller as test apparatus size increases (Weigert, 2001). This uncertainty must be considered with plate sizes of more than 2 m × 2 m in industrial application. Filter plates are often tilted or shaken during cake discharge. In addition, the cake is subject to strong tensile stress before detachment when the plates are moved apart. A tensile adhesion between cake and fabric generates tensile and shear stresses within the cake before shear detachment. Also, it is possible that shear failure and shear breaking within the particulate network occurs (Fränkle et al., 2022). A very stable cake, which is brittle, prevents this scenario.

In summary, the filtration with and the operation of recessed plate filter presses involves understanding of many factors like water content, saturation, adhesion and cohesion as well as their complex interaction. Some of these aspects are known from other fields, for example, behavior of undersaturated filter cakes having a maximum of tensile (Schubert, 1972; Rumpf, 1974; Schubert, 1982) and shear strength (Ozcan et al., 2001; Ozcan et al., 2000; Ozcan et al., 2000) or the description of the saturation kinetics of a particulate networks depending on filtration parameters (Micronics, 2020; VDI, 2017). Tailings are a complex particle system having a broad particle size distribution and consisting of different minerals (Wang et al., 2014) and are not often investigated yet. Furthermore, tailings filtration is a very specific application. For example, a rather short desaturation time is applied to maintain high throughputs resulting in a high residual saturation in mining. Especially, desaturation by pressurized air and its influence is investigated insufficiently for tailings.

Therefore, there are two objectives of this article. The first one is the investigation of the influence of the filtration process parameters filtration pressure, cake thickness as well as gas differential pressure desaturation time and pressure on cake water content, saturation, cake-to-fabric adhesion and cake cohesion. The second one is the development of a mathematical description concerning water content, saturation, cake-to-fabric adhesion and cake cohesion. Thereby, an improved understanding of copper tailings behavior results which simplifies filtration plant operation. Copper tailings are used because they hold an outstanding position in the discussion about tailings, as they are

responsible for nearly half of the global volume of tailings (Baker et al., 2020).

2. Materials and methods

2.1. Copper tailings

FLSmith provided copper tailings as experimental material. A laser scanning microscopy (LSM) image shows the shape of the material with hundredfold magnification in Table 1. Furthermore, significant particle size distribution (PSD) data measured by laser diffraction (HELOS & QUIXEL, Sympatec, Clausthal-Zellerfeld, Germany) is listed. It is assumed that, as typical for tailing applications, a thickening process was applied, however, no information about flocculants is provided. As expected for tailings they have a broad distribution and a high fraction of fines. Density was determined using a gas pycnometer with helium (MultiVolume Pycnometer 1305, Micromeritics Instrument Co., Norcross, USA).

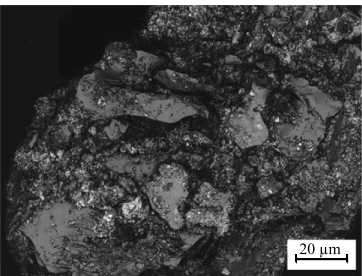
In addition, quantification of the main elements was carried out using wavelength-dispersive X-ray fluorescence (WDXRF) (S4 Explorer, Broker, Bruker Co, Billerica, USA). Results are shown in Table 2. The copper tailings consist mainly of silicon, aluminum, potassium, iron, and calcium.

A further distinction between quartz and other minerals containing silicon is useful since clay minerals have a significant influence on the filtration behavior (Ma et al., 2018). For this reason, a mineralogical analysis was carried out. The results are listed in Table 3. Mineral composition was measured by X-ray diffraction (XRD) (Empyrean, Malvern Panalytical, Malvern, UK). Almost half of the tailings consist of quartz; however, silicon is also present in other silicate minerals like mica, illite, k-feldspar, plagioclase and pyroxene. Mica and illite are phyllosilicates, k-feldspar, plagioclase and quartz are tectosilicates and pyroxene is an inosilicate. Phyllosilicates are also called sheet silicates since they consist of parallel sheets of tetrahedra. Especially swelling clay minerals, for example montmorillonite, which are a certain group of phyllosilicates, hamper filtration (Ma et al., 2018; Grosso et al., 2021).

2.2. Filter cloth

A polypropylene cloth with a satin weave out of monofile fibers was used for filtration experiments. Table 4 shows the main characteristics. This cloth which is suitable for tailings filtration concerning particle retention was used in previous studies on abrasive wear and iron ore lab filtration already. The plastic type reported by the manufacturer was confirmed using wide angle X-ray scattering (WAXS) (Fränkle et al., 2022).

Table 1
LSM image, characteristic PSD data and density of the copper tailings.

Characteristics	Copper tailings
LSM image	
$x_{10,3}/\mu\text{m}$	2.5
$x_{50,3}/\mu\text{m}$	27.4
$x_{90,3}/\mu\text{m}$	144.0
Solid density/ $\text{kg}\cdot\text{m}^{-3}$	2700

2.3. Experimental setup and procedure

A stirred vessel was used for tailings slurry preparation. All filtrations were performed with a slurry solids volume concentration of 30 % solids which replicates thickener underflow. By means of a riser tube compressed air fed the suspension pulsation-free into the same laboratory filter press used in previous publications (Fränkle et al., 2022; Fränkle et al., 2021). It has a cylindrical chamber (100 mm diameter, 40 mm cake height) which is fixed between two end plates. There is a filter medium on each side which was pre-used several times to guarantee constant filtration behavior. Each of the two end plates have a drainage structure and two filtrate outlet pipes, one on top and one on bottom, all equipped with valves. Fig. 1a shows a schematic cross-cut during filtration. The filtrate pipes terminated on a scale that was connected to a process control system (Lab-View, National Instruments, Austin, USA), as were the compressed air supplies and valves.

The two pressure stages tested were 250 kPa and 1250 kPa filtration pressure. This covers a significant part of the tailings pressure filtration application range. After completion of filling, filter cake build-up and compaction by filtration, the valves of the lower filtrate outlet of one end plate and the upper outlet of the other end plate were closed if gas pressure desaturation was applied. Then pressurized air was introduced using the open filtrate outlet on top, as can be seen in Fig. 1b. By overcoming the capillary inlet pressure, the air dewaters the cake by pushing further filtrate out of the open bottom filtrate outlet on the opposite side. 250 kPa and 550 kPa gas differential pressure was used for desaturation. This covers the common range of industrial pressurized air equipment. The following three parameter combinations were investigated: 250 kPa filtration pressure (FP) with 250 kPa air blow (AB), 1250 kPa FP with 250 kPa AB and 1250 kPa FP with 550 kPa AB. For each filtration and air blow pressure combination 0 s, 15 s, 45 s, 90 s and 180 s desaturation time were applied. Thermal drying can be neglected for these desaturation times. In addition, a second chamber thickness of 55 mm was investigated for 250 kPa filtration pressure and 250 kPa air blow pressure for all desaturation times.

The chamber including the filter cake inside and filter cloths still attached was taken out of the filter press after filtration or cake desaturation. Then, the chamber was placed horizontally on an add-on setup for a tensile testing machine. Using a crescent-shaped clamp, as proposed by Ginisty (Ginisty et al., 2016), the filter cloth of the air blow outlet side was pulled off with a velocity of 10 mm min^{-1} and the cake-to-fabric shear adhesion determined, as sketched in Fig. 2a. Assuming a flat filtration area without sealing edge a simplified cake height necessary for detachment can be calculated according to Eq. (2), taking solid and water density as well as cake solid and water content into account.

After the adhesion test, a spacer disc was placed below the filtration chamber, the cake was pushed halfway out of the cylinder and a lid was placed on the upper half of the cake. The tensile testing machine pulled the lid with a velocity of 10 mm min^{-1} and sheared the cake analogues to a Jenike shear cell (ASTM, 2016) (Fig. 2b). The shear strength, also referred to as shear cohesion, was determined by relating the maximum force to the shear area.

Determination of residual filter cake water content was carried out by 24 h thermal drying and weighing. The water content is defined based on the mass of water m_w and the mass of solids m_s according to Eq. (3).

$$\text{Water content} = \frac{m_w}{m_w + m_s} \quad (3)$$

Saturation is calculated, also based on the weight of the filter cake. It is defined based on the volume of water-filled voids $V_{v, \text{water-filled}}$ and the total voids volume $V_{v, \text{total}}$, which are completely water-filled after filtration, according to Eq. (4).

$$S = \frac{V_{v, \text{water-filled}}}{V_{v, \text{total}}} \quad (4)$$

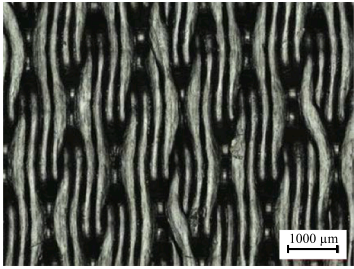
Table 2
Main elements of the copper tailings measured by WDXRF.

Na	Mg	Al	Si	P	K	Ca	Ti	Mn	Fe	LOI
1 %	2 %	10 %	65 %	<1%	8 %	4 %	1 %	<1%	5 %	4 %

Table 3
XRD mineralogy analysis results of the copper tailings.

Mica	Gypsum	Illite	K-felspar	Plagioclase	Pyroxene	Quartz
7.9	2.6	4.0	27.5	6.5	3.6	48.1

Table 4
LSM image of the filter cloth and characteristics (Fränkle et al., 2022).

Characteristics	Copper tailings
LSM image	
Material	Polypropylen
Weave type	Satin
Fiber type	Monofile & monofile
Unused flow resistance/m ⁻¹	2.6 ± 0.6 × 10 ⁸

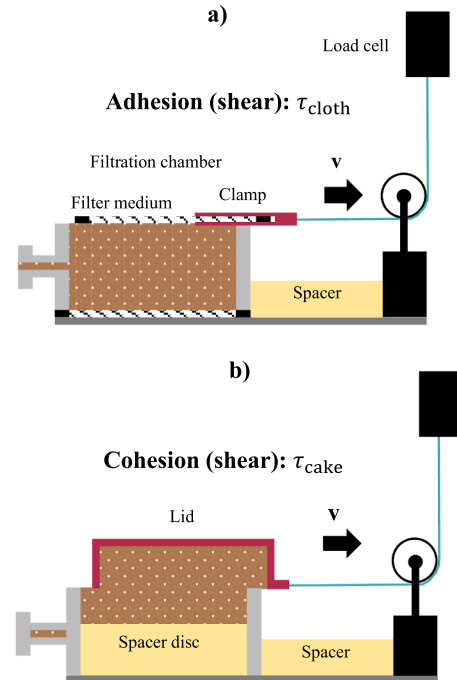


Fig. 2. Schematic cross-cuts of filter cake-to-fabric shear adhesion (a) and cake shear cohesion (b) measurements (Fränkle et al., 2022).

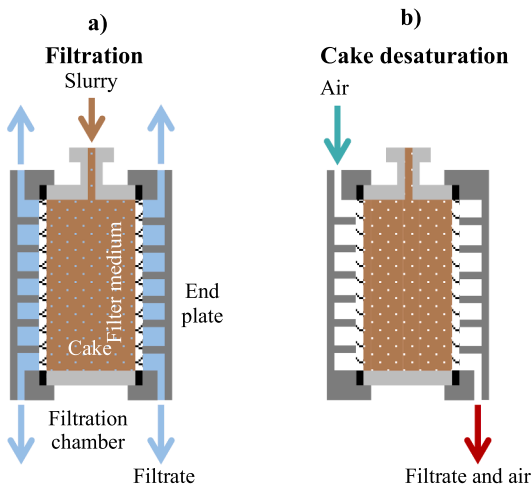


Fig. 1. Schematic cross-cut of the lab filter press filtration and the cylindric filtration chamber during filtration (a) and cake desaturation (b) (Fränkle et al., 2022).

The loss of liquid during desaturation was related to the average amount of liquid in a cake resulting from the same filtration pressure without desaturation.

2.4. Mathematical model

In addition to measurement of the influence of gas differential pressure desaturation on water content, cake saturation, cake-to-fabric shear adhesion and filter cake shear cohesion, another objective of this work is the development of a simplified mathematical model. It is supposed to describe the mentioned quantities for different filtration

pressures, gas differential pressures and desaturation times in sufficient accuracy. In conjunction with the experimental setup described, it is intended to enable tailings behavior prediction with a small number of tests on site.

Some assumptions are made for this purpose and their justification is discussed in the results and discussion section. These facilitate the handling compared to existing approaches, e.g., for the description of saturation kinetics by Nicolaou (Fig. 1) (VDI, 2017; Nicolaou, 1999). His approach is useful in filtration engineering because it measures all relevant parameters during standard tests. However, this is randomly the case for tailings filtration. Therefore, a more holistic approach is proposed in this article to describe water content, cake saturation, cake-to-fabric shear adhesion and filter cake shear cohesion kinetics during air blow desaturation. A list of all assumptions can be found in the Appendix.

The first assumption is that the time-dependent kinetics of the above quantities is a constrained growth or decrease and can be described by an exponential function according to Eq. (5). While this is justified for residual cake water content and saturation, the literature for adhesion and cohesion shows a different behavior when considering the complete saturation range from 0 to 1. However, since desaturation of tailings filter cake only occurs within a high range of saturation, the assumption is plausible. $x(t)_{ij}$ is the quantity, $x_{i,j,\infty}$ the value at equilibrium, $x_{i,j,0}$ the initial value and $a_{i,j,h}$ the kinetics parameter. The indices of the time-dependent quantity i and j stand for the filtration pressure and air blow pressure, respectively. h states the cake height.

$$x(t)_{ij} = x_{i,j,\infty} - (x_{i,j,\infty} - x_{i,j,0}) \cdot e^{-a_{i,j,h} \cdot t} \tag{5}$$

Furthermore, the initial value of the quantity is invariable, for example the cohesion of the saturated filter cake would be $cohesion_{i,j,0}$.

The value of the fitted curve $x_{i,j,0}$ at that time is similar to the measured value $\hat{x}_{i,j,0}$ (see Eq. (6)). This is the second assumption.

$$x_{i,j,0} = \hat{x}_{i,j,0} \tag{6}$$

Assumption three is that $a_{i,j,h}$ is one of two fit parameters. It describes how fast the increase or decrease caused by desaturation. As shown in Eq. (7), it is specific for every combination of filtration pressure, air blow pressure and cake thickness.

$$a_{1,1,1} \neq a_{2,1,1} \neq a_{2,2,1} \tag{7}$$

$x_{i,j,\infty}$ is the second fit parameter. It determines the limit of the constrained growth. However, it is specified that it depends only on the air blow pressure not on the filtration pressure for a certain cake thickness. This fourth assumption implicates Eq. (8).

$$x_{1,j,\infty} = x_{2,j,\infty} \tag{8}$$

Concerning the tests in this study, in which 250 kPa air blow is performed for both filtration pressures, one average value at equilibrium is used for both.

Assumption five states, that 180 s is sufficient close to the saturation value at equilibrium for a specific air blow concerning a cake thickness of 40 mm and, thus, the ratio of a quantity resulting by two different air blow pressures is the same as for 180 s, according to Eq. (9).

$$\frac{x_{i,2,\infty}}{x_{i,1,\infty}} = \frac{x_{i,2,180}}{x_{i,1,180}} = \frac{x_{1250,550,180s}}{0.5 \cdot (x_{250,250,180s} + x_{1250,250,180s})} = const. \tag{9}$$

The two fit parameters for the present data are determined by minimizing the sum of square residuals for all three, according to Eq. (10).

$$\min_{a_{i,j,h}; x_{i,j,\infty}} S = \sum_{k=1}^n (x_{1,1,k} - \hat{x}_{1,1,k})^2 + \sum_{k=1}^n (x_{2,1,k} - \hat{x}_{2,1,k})^2 + \sum_{k=1}^n (x_{2,2,k} - \hat{x}_{2,2,k})^2 \tag{10}$$

Another aspect of this article is to compare the behavior of the standard cake thickness of 40 mm and a thicker cake of 55 mm. According to Anlauf, the desaturation process differs only in its kinetics (Anlauf, 2019). Therefore, the $x_{i,j,0}$ and $x_{i,j,\infty}$ values of the thinner cake are adopted for the mathematical modeling of the thicker cake.

3. Results and discussion

The authors of this article assume t-distributed data. All charts give the estimated mean values and, in addition, the range of the 50 % confidence level. Furthermore, the application of the modeling approach described above results in the fitted curves. The corresponding tables in the Appendix list the fit parameters. In general, the description of constrained growth or decrease meets the data with sufficient accuracy given the underlying assumptions. This justifies these simplifications.

As mentioned, no information about flocculants was provided for the copper tailings. However, flocculants are commonly used to enhance the performance of gravity thickeners in systems with fine particles and play a crucial role in tailings processing (Jewell and Fourie, 2015). Moreover, they significantly influence filtration kinetics (Alam et al., 2011). This limitation impacts the transferability of the results to some extent.

3.1. Filtration pressure and air blow pressure influence

Results of the water content for different filtration and air blow pressures over various desaturation times are shown in Fig. 3. Since the two filtration pressures result in a different compression of the particulate network, the cake water content for fully saturated filter cake, i.e., at a desaturation time of 0 s, is slightly lower for 1250 kPa filtration. Since these two filtration pressures approximately cover the range of technically applied filtration pressures in recessed plate filter presses, it

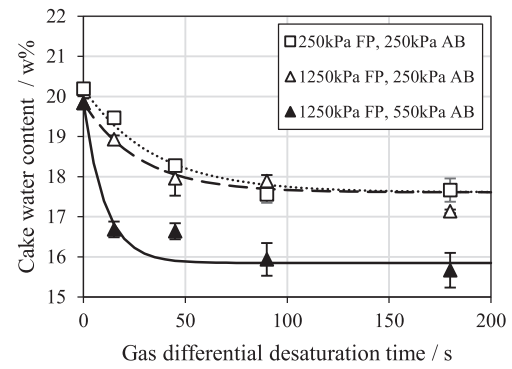


Fig. 3. Filter cake water content of each filtration pressure and air blow pressure combination for variation of the desaturation time for a cake thickness of 40 mm.

is apparent that filtration without post-treatment limits the achievement of low residual water contents. By applying pressurized air desaturations, a significant further decrease in cake water content can be seen for all combinations of filtration and desaturation pressure. Especially for a high air blow pressure there is a strong decrease within a short time. However, the desaturation effect decreases with higher air blow application time. The water content approaches the value at equilibrium for the corresponding pressure at 90 s desaturation time for the investigated cake height of 40 mm. As assumed, it is a constrained decrease. A considerable amount of water remains within the cake due to isolated pores having higher capillary inlet pressures than the air blow pressure applied (Anlauf, 2019). Overall, water content is reduced from approximately 20 w% to below 18 w% for 250 kPa and below 16 w% for 550 kPa air blow pressure by 180 s gas differential pressure desaturation. The intensity of the air blows is obviously the decisive variable for setting the residual water content. 550 kPa doubles the additional reduction in relation to filtration compared to 250 kPa.

Parameters of the water content fitted curves are listed in the Appendix. For the fits, the estimated value at equilibrium based on a ratio of 0.9004 is 17.61 w% for 250 kPa AB and 15.85 w% for 550 kPa AB. For a filter cake of 40 mm, mechanical desaturation and, therefore, filter cake desaturation mainly takes place in the first 90 s of air blow.

In general, saturation values behave analogous to the water content data for application of air blow. Data are given in Fig. 4. In contrast to the water content, saturation curves for all three filtration and air blow pressure combination start at the full saturation of 100 v% since the corresponding unsaturated cake is the reference for each of them. Air blow decreases pore saturation for all combinations of filtration and

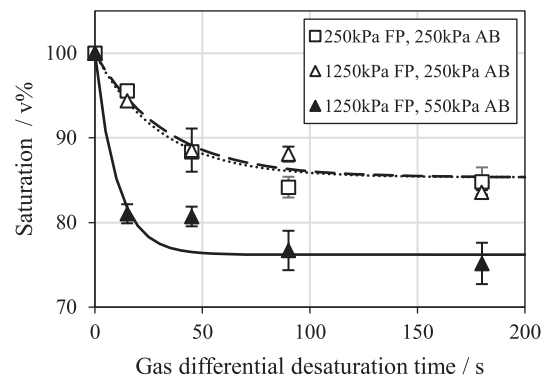


Fig. 4. Filter cake saturation of each filtration pressure and air blow pressure combination for variation of the desaturation time for a cake thickness of 40 mm.

desaturation pressure in a constrained decrease. A higher air blow pressure results in a stronger decrease and a lower final range for longer air blow times, whereas both data curves for 250 kPa air blow are nearly similar in trend. This supports the statement that the gas differential pressure is the decisive parameter for a slightly compressible filter cake. The mechanical desaturation limit due to isolated pores can be stated to be approx. 84 v% using 250 kPa and 75 v% applying 550 kPa desaturation pressure.

The Appendix section gives all parameters of the fitted saturation curves. Analogous to the cake water content, the value at equilibrium is reached within 60 to 90 s. This timeframe falls within the application times investigated, and the mathematical model is close to the measurements despite the simplifications. Fit values at equilibrium are 85.33 v% for 250 kPa AB and 76.20 v% for 550 kPa. The ratio is set at 0.8928.

Fig. 5 shows the cake-to-fabric shear adhesion at different desaturation times for each combination of filtration and desaturation pressure. In contrast to water content and saturation, filter cake adhesion is a constrained growth in the investigated saturation range. Filtration without cake post-treatment results in the lowest filter cake adhesion at 0 s air blow time. A higher compaction of the cake, based on a higher filtration pressure, results in a higher initial adhesion. At short desaturation times adhesion increases strongly. The effect is more distinct for the high air blow pressure. By trending towards the value at equilibrium a flattening of the curve can be seen with higher air blow times analogous to the water content and saturation. The adhesion value at 180 s is only slightly higher for 550 kPa with 3.1 kN m^{-2} than for 250 kPa air blow with 2.9 kN m^{-2} (550 kPa AB) and 2.5 kN m^{-2} (250 kPa AB). In comparison to the corresponding fully saturated cake at 0 s air blow adhesion doubles approximately for a 1250 kPa filter cake desaturated 180 s at 550 kPa air blow and triples approximately for a 250 kPa filter cake desaturated 180 s at 250 kPa air blow. Consequently, the increase in adhesion raises the necessary cake thickness for gravity-based detachment significantly. Corresponding cake thicknesses, calculated according to Eq. (2), are given by the second y-axis. This increase complicates the desired cake detachment, especially since the cake thicknesses are larger than usual chamber dimensions of 30–60 mm for mining applications (Outotec, 2022). However, adhesion measurements are strongly affected by the measurement system as well as dimensions and cake detachment might be observed for smaller thicknesses as mentioned in the introduction section (Fränkle et al., 2022; Weigert and Ripperger, 1997).

Adhesion fit parameters are listed in the Appendix. Based on a ratio of 1.1349 estimated value at equilibrium is 2.787 kN m^{-2} for 250 kPa AB and 3.150 kN m^{-2} for 550 kPa AB. Adhesion increase reaches the equilibrium for shorter desaturation time in comparison to water content and saturation.

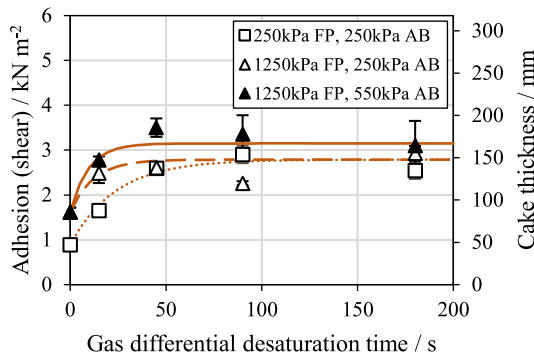


Fig. 5. Filter cake shear adhesion and calculated corresponding cake height for gravity introduced detachment of each filtration pressure and air blow pressure combination for variation of the desaturation time for a cake thickness of 40 mm.

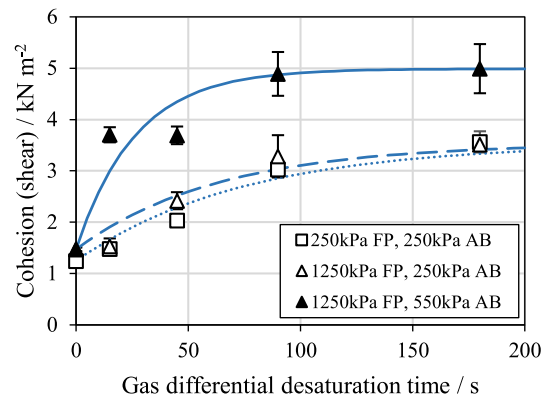


Fig. 6. Filter cake shear cohesion of each filtration pressure and air blow pressure combination for variation of the desaturation time for a cake thickness of 40 mm.

Measurements of filter cake shear cohesion, which is similar to shear strength, are plotted in Fig. 6. Analogous to the adhesion, the cohesion of the fully saturated filter cake starts at relatively low values and is a constrained growth in the investigated desaturation range. Evaluating the data points at 0 s air blow time leads to the finding that particulate structures which are more compressed due to higher filtration pressure have a slightly higher cohesion. Compared to the adhesion, cohesion of fully saturated filter cakes is in the same range between 1 and 2 kN m^{-2} . By pressurized air desaturation shear strength increases for each combination of filtration and air blow pressure investigated. Concerning the time which the desaturation is applied, there is an increase within the first two minutes. Afterwards the cohesion is approaching the value at equilibrium. Values at 180 s desaturation are 3.6 kN m^{-2} (250 kPa FP, 250 kPa AB), 3.5 kN m^{-2} (1250 kPa FP, 250 kPa AB) and 5.0 kN m^{-2} (1250 kPa FP, 550 kPa AB). Compared to the fully saturated state shear cohesion more than triples for a 1250 kPa filter cake desaturated 180 s at 550 kPa air blow and nearly triples for a 250 kPa filter cake desaturated 180 s at 250 kPa air blow.

Parameters of the fitted shear cohesion curves are given in the Appendix. The value at equilibrium is reached within the application times investigated, analogous to the shear adhesion, however, it takes longer. There is an acceptable deviation between fitted curves and measurements justifying the assumptions of the model. Values at equilibrium are 3.538 kN m^{-2} for 250 kPa AB and 4.989 kN m^{-2} for 550 kPa. The ratio is set at 1.4101.

In addition, the ratio of adhesion and cohesion is an important point

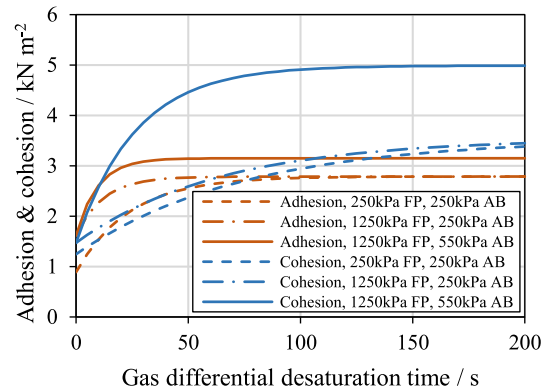


Fig. 7. Cake-to-fabric adhesion and cake shear cohesion fits of each filtration pressure and air blow pressure combination for variation of the desaturation time for a cake thickness of 40 mm.

for cake detachment. Adhesion should be as low as possible, while cohesion should be as high as possible (Weigert, 2001). Fig. 7 shows all the adhesion and cohesion fits from the previous figures. A Comparison of the curves for both quantities at the same filtration and air blow pressure indicates that adhesion kinetics are faster than cohesion kinetics. After 60 s each adhesion curve is close to the value at equilibrium, whereas cohesion curves need approximately 120 s for 40 mm cakes. Based on these findings a recommendation for plant operation can be stated: There is supposed to be a trade-off between longer desaturation time associated with lower throughput and easier detachment linked to shorter technical downtimes caused by cake sticking and breakage.

In addition, all adhesion and cohesion measurements related to water content and saturation are presented in the Appendix. Adhesion increases with lower water content as well as decreasing saturation; however, the trend flattens as these values decrease. Cohesion also increases with lower water content and lower saturation but, unlike adhesion, this behavior remains consistent across the entire range of investigated water content and saturation level. It can be concluded that the cohesion-to-adhesion ratio increases as dewatering becomes more intense through desaturation.

3.2. Filter cake thickness

Besides the detailed investigation for 40 mm filter cakes, tests with a second cake thickness of 55 mm were carried out for 250 kPa filtration pressure and 250 kPa air blow to evaluate changes in kinetics. Anlauf states that thicker cakes have the same values at equilibrium for identical filtration and air blow pressure stages (Anlauf, 2019). Therefore, equilibrium and initial values are set identical to tests with 40 mm cake thickness. Only the kinetics parameter $a_{i,j,h}$ is allowed to change. Fig. 8 shows water content of the 40 mm and 55 mm filter cakes for different air blow times. Furthermore, fitted curves according to the mathematical model presented and restrictions mentioned are given. As expected, the desaturation takes more time for the thicker cake. Overall, the effect is small for the variation investigated. The value at equilibrium is reached after 180 s instead of 90 s. Despite an increase in cake thickness of 37.5 % the in time needed for desaturation doubles. Based on the flattening of the curve the kinetics parameter decreases as can be seen in the Appendix.

Saturation, shear adhesion and shear cohesion of the 55 mm filter cakes including the corresponding 40 mm filter cake values are shown in the Appendix. In addition, the corresponding kinetics parameters of the fitted curves are listed. The desaturation of the 55 mm cakes behaves similarly to the water content. Desaturation takes longer compared to

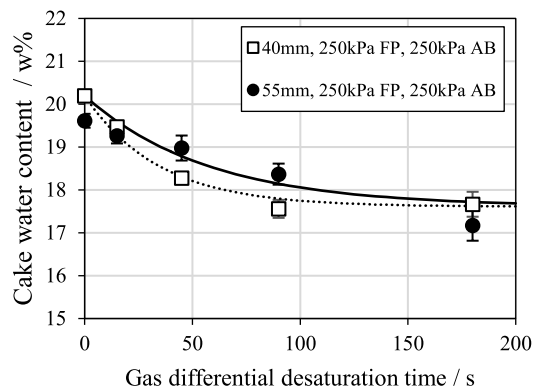


Fig. 8. Filter cake water content of 250 kPa filtration pressure and 250 kPa air blow pressure combination for variation of the desaturation time for cake thicknesses of 40 and 55 mm.

the 40 mm cake thickness and reaches the value at equilibrium after approximately 180 s. Also, shear adhesion increase is slower for thicker cakes, maximum values lie between 2 and 3 kN m^{-2} for the time range investigated. However, there is a delay in increase since the adhesion is measured on the opposite site of the pressurized air application (right-hand filter cloth, see Fig. 1b) and 15 s are not sufficient to start desaturation within the whole cake thickness. Higher initial adhesion values are correlated to an ongoing blinding of the cloth. Shear cohesion values of the 55 mm cakes are close to the data of the 40 mm cakes since shear cohesion is measured in the middle of the cake, which is 27.5 mm and 20 mm. Therefore, it is quite similar. Further research concerning cake thicknesses should include detailed investigations into area-specific air flow rates, overall air consumption, and operational costs.

3.3. Filter cake characteristics

It stands out that slight changes in compaction and, especially, application of desaturation result in decrease of water content in copper tailings filter cakes. In contrast, desaturation generates enormous increase in adhesion as well as cohesion and, therefore, appearance and behavior of the particulate network. This is illustrated by exemplary pictures of filter cakes in Fig. 9 which were taken after the shear cohesion tests. Additional stress applied by taking the cakes out of the test rig and placing them into dishes for drying results in dynamic liquefaction for the wetter cakes, e.g., 250 kPa filtration cakes without desaturation, as can be seen in Fig. 9a. This behavior can be explained by the fact that, in terms of the Atterberg limits, these cakes are still able to flow. In soil mechanics and geotechnical engineering, this is referred to as the established liquid limit. This limit marks the transition from being able to flow to plastic behavior and is defined as a particulate network cohesion of about 2 kPa (Jewell and Fourie, 2015; ASTM, 2018). The tailings filter cakes without post-treatment in this study have shear strengths of 1.2 kN m^{-2} (250 kPa filtration pressure) and 1.4 kN m^{-2} (1250 kPa filtration pressure). Desaturated filter cakes behave more brittle and maintain their shape. This characteristic is illustrated in Fig. 9b, where a filter cake, produced under a filtration pressure of 1250 kPa and subjected to 180 s air blow at 550 kPa, exhibits these properties, having an average shear cohesion of 5.0 kN m^{-2} .

4. Conclusions

The first objective of this article was to investigate the influence of filtration pressure, air blow desaturation time, air blow pressure and cake thickness on copper tailings filter cake water content, saturation, cake-to-fabric adhesion and filter cake cohesion. Therefore, filtration, shear adhesion and shear cohesion tests were carried out using copper tailings, a laboratory filter press and a specially adapted shear test rig in a modified tensile testing machine. The setup enables direct force measurements on the particulate network (filter cake) after filtration or air blow post-treatment. Thus, it generates a benefit in filtration lab test work regarding investigation of the adhesion and cohesion and their effect on the filtration process. This is of major importance considering maintenance of high throughputs in recessed plate filter presses, i.e., successful cake detachment, and geotechnical stability concerns for subsequent stacking.

In detail, a study of cake desaturation was carried out regarding desaturation pressure and desaturation time variation for two filtration pressures, two air blow pressures and two cake thicknesses. For the same cake thickness, a higher filtration pressure results in a slightly lower water content, higher cake-to-fabric adhesion and higher cohesion. However, slight compressibility of the copper tailings limits significant improvement of the dewatering by filtration pressure increase only. Thereof, adhesion and cohesion increase are also small without cake post-treatment. However, applying desaturation after filtration by pressurized air (air blow) leads to a significant decrease in water content and saturation and increase in adhesion and cohesion instantaneously.

a)



b)



Fig. 9. Example of two 40 mm filter cakes: (a) 250 kPa filtration pressure, no air blow, average water content 20.2 w%, saturation 100 v%, average shear adhesion 0.9 kN m^{-2} , average shear cohesion 1.2 kN m^{-2} ; (b) 1250 kPa filtration pressure, 180 s air blow, 550 kPa air blow pressure, average water content 15.7 w%, average saturation 75 v%, average shear adhesion 3.1 kN m^{-2} , average shear cohesion 5.0 kN m^{-2} .

Since the kinetics behave as a constrained decrease or constrained growth, longer desaturation times enhance the effect up to a certain value at equilibrium. The range of the equilibrium is mainly dependent on the air blow pressure. In detail, a higher desaturation pressure generates a lower water content, a higher adhesion, and a higher cohesion for an identical filtration pressure. Furthermore, desaturation increases more sharply at the beginning for a higher air blow pressure. Thicker

cakes need longer desaturation times. A mathematical model proposed describes the measurements sufficiently and its assumptions turned out to be justified.

It can be stated that desaturation is beneficial for cake detachment in two ways: Cohesion increases, i.e., the filter cakes are unable to flow, behave more brittle and maintain their shape. Furthermore, longer desaturation times increase cohesion more than adhesion. Therefore, it

is more likely to detach the filter cake completely as a whole. Lower throughputs by longer desaturation times are supposed to reduce technical downtime, e.g., for filter fabric surface cleaning. In addition, a higher air blow pressure enhances the final ratio between shear cohesion and shear adhesion which can be reached by mechanical desaturation.

The presented measurement methodologies and mathematical model support the design and operation of tailings filtration plants by estimating the behavior of the particulate network with sufficient accuracy. For example, this approach facilitates the design of new filtration plants by assessing the feasibility of various process parameter combinations (e.g., filtration pressure, air blow pressure, air blow time, and cake height) to achieve certain target values of cake properties. It also enables the modeling of process time and area-specific throughput for each possible combination. Additionally, by comparing costs of different process parameter combinations and filtration area (size and number of filter presses, number of plates per press) for a required plant throughput, the most economical solution can be realized. For existing plants, especially those that are bottlenecks, optimizing throughput through process parameter adjustments can enhance overall performance for the given filtration area.

CRedit authorship contribution statement

Bernd Fränkle: Writing – review & editing, Writing – original draft,

Visualization, Methodology, Investigation, Data curation, Conceptualization. **Thien Sok:** Supervision. **Marco Gleiß:** Supervision. **Hermann Nirschl:** Supervision, Funding acquisition.

Declaration of competing interest

The authors declare the following financial interests/personal relationships which may be considered as potential competing interests: This work was sponsored by FLSmidth.

Data availability

The authors do not have permission to share data.

Acknowledgements

The authors would like to thank all students and colleagues who have contributed to the successful completion of this work. Special thanks for support go to Michael Madsen, James Chaponnel, Scott Reddick, Dave Hanfland, Paul McCurdie, Todd Wisdom, Brent Stokes and Steve Ware from FLSmidth. The regular meetings and critical discussions have contributed significantly to the success of the work. This work was sponsored by FLSmidth.

Appendix A

Table A1

Assumptions for the mathematical model.

No.	Equation	Description
1	$x(t)_{ij} = x_{ij,\infty} - (x_{ij,\infty} - x_{ij,0}) \cdot e^{-a_{ij,h} \cdot t}$	Time-dependent kinetics of the quantities (cake water content, saturation, adhesion, or cohesion) is a constrained growth or decrease and can be described by an exponential function. $x(t)_{ij}$ is the quantity, $x_{ij,\infty}$ the value at equilibrium, $x_{ij,0}$ the initial value and $a_{ij,h}$ the kinetics parameter. Indices of the time-dependent quantity i and j stand for the filtration pressure and air blow pressure, respectively. h states the cake height. Only $a_{ij,h}$ is affected by cake height variation.
2	$x_{ij,0} = \hat{x}_{ij,0}$	Value of the fitted curve $x_{ij,0}$ at 0 s is similar to the measured value $\hat{x}_{ij,0}$ at 0 s.
3	$a_{1,1,1} \neq a_{2,1,1} \neq a_{2,2,1}$	$a_{ij,h}$ is one of two fit parameters. It describes how fast the increase or decrease caused by desaturation. It is specific for every combination of filtration pressure, air blow pressure and cake thickness.
4	$x_{1,j,\infty} = x_{2,j,\infty}$	$x_{ij,\infty}$ is the second fit parameter. It determines the limit of the constrained growth. It is specified that it depends only on the air blow pressure not on the filtration pressure for a certain cake thickness.
5	$\frac{x_{1,2,\infty}}{x_{1,1,\infty}} = \frac{x_{1,2,180s}}{x_{1,1,180s}} = \frac{x_{1250,550,180s}}{0.5 \cdot (x_{250,250,180s} + x_{1250,250,180s})} = const.$	180 s is sufficient close to the saturation value at equilibrium for a specific air blow concerning a cake thickness of 40 mm. Thus, the ratio of a quantity resulting by two different air blow pressures is the same as for 180 s.
6	$\min_{a_{ij,h}; x_{ij,\infty}} S = \sum_{k=1}^n (x_{1,1,k} - \hat{x}_{1,1,k})^2 + \sum_{k=1}^n (x_{2,1,k} - \hat{x}_{2,1,k})^2 + \sum_{k=1}^n (x_{2,2,k} - \hat{x}_{2,2,k})^2$	The two fit parameters for the present data are determined by minimizing the sum of square residuals for all three curves.

Appendix B

Table B1

Fit parameter of water content modeling for a cake thickness of 40 mm.

Combination	Parameter	Value
250 kPa FP, 250 kPa AB, 40 mm	Water content _{250,250,0}	20.20
	Water content _{250,250,∞}	17.61
	$a_{250,250,40}$	0.02917
1250 kPa FP, 250 kPa AB, 40 mm	Water content _{1250,250,0}	19.84
	Water content _{1250,250,∞}	17.61
	$a_{1250,250,40}$	0.03603
1250 kPa FP, 550 kPa AB, 40 mm	Water content _{1250,550,0}	19.84
	Water content _{1250,550,∞}	15.85

(continued on next page)

Table B1 (continued)

Combination	Parameter	Value
$x_{i,j,\infty}$ ratio	$a_{1250,550,40}$	0.09449
	$Water\ content_{1250,550,180s}$	0.9004
	$0.5 \cdot (Water\ content_{250,250,180s} + Water\ content_{1250,250,180s})$	

Table B2

Fit parameter of saturation modeling for a cake thickness of 40 mm.

Combination	Parameter	Value
250 kPa FP, 250 kPa AB, 40 mm	$Saturation_{250,250,0}$	100
	$Saturation_{250,250,\infty}$	85.33
	$a_{250,250,40}$	0.03308
1250 kPa FP, 250 kPa AB, 40 mm	$Saturation_{1250,250,0}$	100
	$Saturation_{1250,250,\infty}$	85.33
	$a_{1250,250,40}$	0.03008
1250 kPa FP, 550 kPa AB, 40 mm	$Saturation_{1250,550,0}$	100
	$Saturation_{1250,550,\infty}$	76.20
	$a_{1250,550,40}$	0.09752
$x_{i,j,\infty}$ ratio	$Saturation_{1250,550,180s}$	0.8928
	$0.5 \cdot (Saturation_{250,250,180s} + Saturation_{1250,250,180s})$	

Table B3

Fit parameter of shear adhesion modeling for a cake thickness of 40 mm.

Combination	Parameter	Value
250 kPa FP, 250 kPa AB, 40 mm	$Adhesion_{250,250,0}$	0.890
	$Adhesion_{250,250,\infty}$	2.787
	$a_{250,250,40}$	0.04196
1250 kPa FP, 250 kPa AB, 40 mm	$Adhesion_{1250,250,0}$	1.617
	$Adhesion_{1250,250,\infty}$	2.787
	$a_{1250,250,40}$	0.08254
1250 kPa FP, 550 kPa AB, 40 mm	$Adhesion_{1250,550,0}$	1.617
	$Adhesion_{1250,550,\infty}$	3.150
	$a_{1250,550,40}$	0.10426
$x_{i,j,\infty}$ ratio	$Adhesion_{1250,550,180s}$	1.1349
	$0.5 \cdot (Adhesion_{250,250,180s} + Adhesion_{1250,250,180s})$	

Table B4

Fit parameter of shear cohesion modeling for a cake thickness of 40 mm.

Combination	Parameter	Value
250 kPa FP, 250 kPa AB, 40 mm	$Cohesion_{250,250,0}$	1.245
	$Cohesion_{250,250,\infty}$	3.538
	$a_{250,250,40}$	0.01346
1250 kPa FP, 250 kPa AB, 40 mm	$Cohesion_{1250,250,0}$	1.471
	$Cohesion_{1250,250,\infty}$	3.538
	$a_{1250,250,40}$	0.01565
1250 kPa FP, 550 kPa AB, 40 mm	$Cohesion_{1250,550,0}$	1.471
	$Cohesion_{1250,550,\infty}$	4.989
	$a_{1250,550,40}$	0.03995
$x_{i,j,\infty}$ ratio	$Cohesion_{1250,550,180s}$	1.4101
	$0.5 \cdot (Cohesion_{250,250,180s} + Cohesion_{1250,250,180s})$	

Appendix C

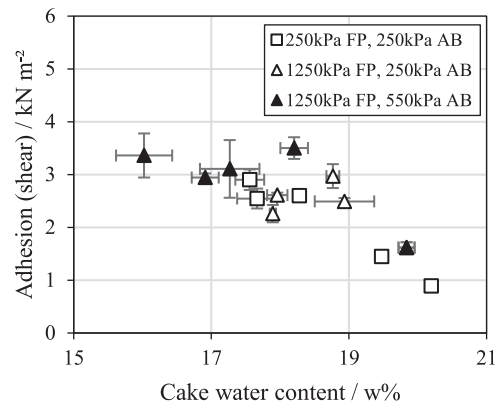


Fig. C1. Cake-to-fabric shear adhesion of all 40°-mm cake height measurements over cake water content.

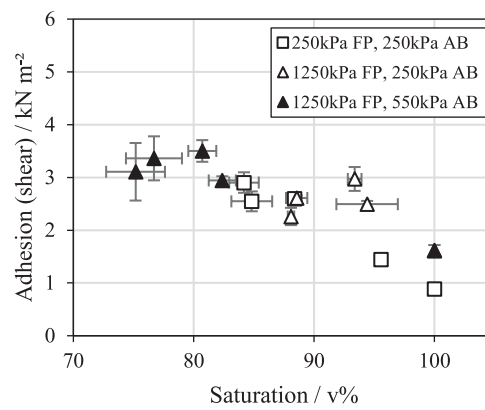


Fig. C2. Cake-to-fabric shear adhesion of all 40°-mm cake height measurements over cake saturation.

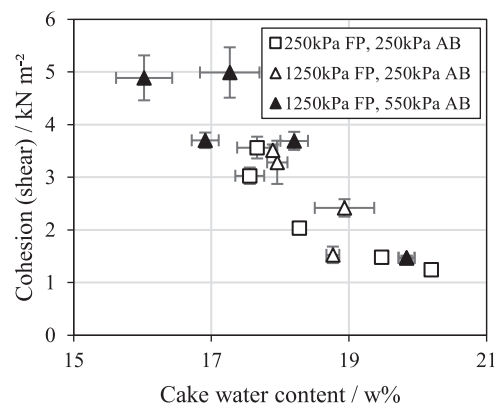


Fig. C3. Cake shear cohesion of all 40°-mm cake height measurements over cake water content.

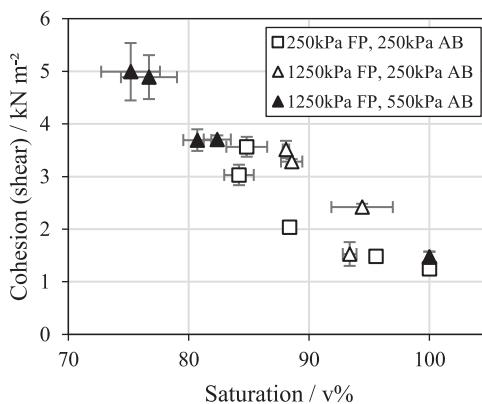


Fig. C4. Cake shear cohesion of all 40° mm cake height measurements over cake saturation.

Appendix D

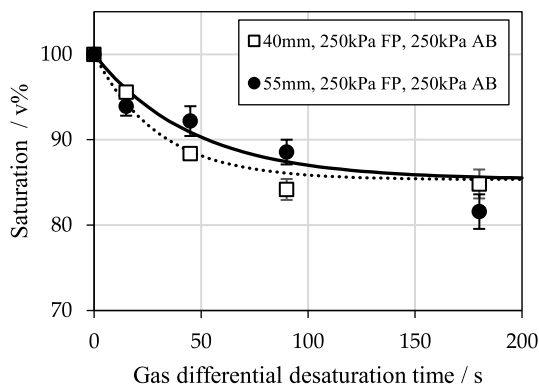


Fig. D1. Filter cake saturation of 250 kPa filtration pressure and 250 kPa air blow pressure combination for variation of the desaturation time for cake thicknesses of 40 and 55 mm.

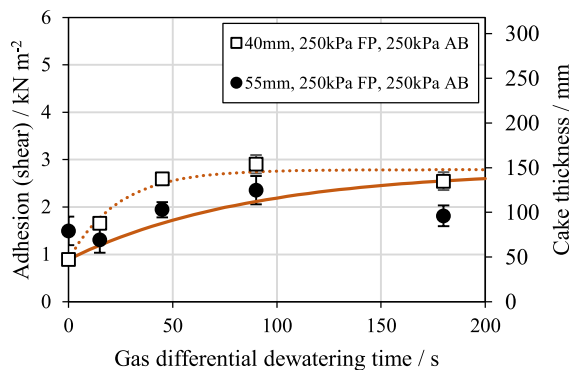


Fig. D2. Filter cake-to-fabric shear adhesion of 250 kPa filtration pressure and 250 kPa air blow pressure combination for variation of the desaturation time for cake thicknesses of 40 and 55 mm.

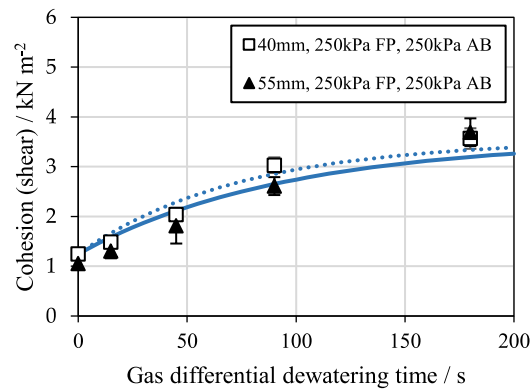


Fig. D3. Filter cake shear cohesion of 250 kPa filtration pressure and 250 kPa air blow pressure combination for variation of the desaturation time for cake thicknesses of 40 and 55 mm.

Table D1

Fit parameter of water content modeling for a cake thickness of 55 mm.

Combination	Parameter	Value
250 kPa FP, 250 kPa AB, 55 mm	$Water\ content_{250,250,0}$	20.20
	$Water\ content_{250,250,\infty}$	17.61
	$a_{250,250,55}$	0.01752

Table D2

Fit parameter of saturation modeling for a cake thickness of 55 mm.

Combination	Parameter	Value
250 kPa FP, 250 kPa AB, 55 mm	$Saturation_{250,250,0}$	100
	$Saturation_{250,250,\infty}$	85.33
	$a_{250,250,55}$	0.01375

Table D3

Fit parameter of filter fabric to filter cake shear adhesion modeling for a cake thickness of 55 mm.

Combination	Parameter	Value
250 kPa FP, 250 kPa AB, 55 mm	$Adhesion_{250,250,0}$	0.890
	$Adhesion_{250,250,\infty}$	2.787
	$a_{250,250,55}$	0.01156

Table D4

Fit parameter of shear cohesion modeling for a cake thickness of 55 mm.

Combination	Parameter	Value
250 kPa FP, 250 kPa AB, 55 mm	$Cohesion_{250,250,0}$	1.245
	$Cohesion_{250,250,\infty}$	3.538
	$a_{250,250,55}$	0.01057

References

Alam, N., Ozdemir, O., Hampton, M., Nguyen, A., 2011. Dewatering of coal plant tailings: flocculation followed by filtration. *Fuel* 90 (1), 26–35.

Anlauf, H., 2019. *Wet Cake Filtration - Fundamentals, Equipment, and Strategies*. Wiley-VCH Verlag, Weinheim.

ASTM, 2016. ASTM D6128–16; Standard Test Method for Shear Testing of Bulk Solids Using the Jenike Shear Tester. ASTM International, West Conshohocken.

ASTM, 2018. ASTM D4318-17e1; Standard Test Method for Liquid Limit, Plastic Limit, and Plasticity Index of Soils. ASTM International, West Conshohocken.

Baker, E., Davies, M., Fourie, A., Mudd, G., Thygesen, K., 2020. Mine tailings facilities: overview and industry trends in towards zero harm - a compendium of papers

prepared for the global tailings review. In: Oberle, B., Brereton, D., Mihaylova, A. (Eds.) *Global Tailings Review*, London.

Blanchet, N., 2018. Use of statistical approach in tailings filtration: learnings from cloth failures. In: *Proceeding of Alumina Conference*, Gladstone.

Bleiwass, D., 2012. *Estimated Water Requirements For the Conventional Flotation of Copper Ores*. U.S. Geological Survey Open-File Report. U.S Geological Survey, Ranson.

Bustillo Revuelta, M., 2017. *Mineral Resources - From Exploration to Sustainability Assessment*. Springer International Publishing AG, Cham.

Concha, F.A., 2014. *Fluid Mechanics and Its Applications - Solid-Liquid Separation in the Mining Industry*. Springer International Publishing Switzerland, Cham.

- Das, T., Usher, S., Batstone, D., Othman, M., Rees, C., Stickland, A., Eshtiagi, N., 2023. Impact of volatile solids destruction on the shear and solid-liquid separation behaviour of anaerobic digested Sludge. *Sci. Total Environ.* 164546.
- Davies, M., Rice, S., 2001. An Alternative to conventional tailing management - dry stack. In: *Proceedings of the Tailings and MineWaste Conference, Vancouver*.
- Davies, M., 2011. Filtered dry stacked tailings – the fundamentals. In: *Proceedings Tailings and Mine Waste, Vancouver, 2011*.
- FLSmidth Minerals Technology Center, 2012. EIMCO® Colossal™ Automatic Filter Press (AFP). [Online]. Available: https://www.flsmidth.com/-/media/brochures/brochure-res-products/filtration/pressure-filters/colossalfilterpress_brochure_email.pdf. [Accessed 24 July 2023].
- FLSmidth Minerals Technology Center, 2019. Tailings Management - Sustainable and Complete Dewatering Solutions. [Online]. Available: <https://www.flsmidth.com/-/media/brochures/brochures-solutions/2019/fls-tailings-management-brochure-web-20190503.pdf>. [Accessed 23 June 2023].
- Fränkle, B., Morsch, P., Nirschl, H., 2021. Towards prediction of cake detachment in tailings filtration. In: *Paste 2021: 24th International Conference on Paste, Thickened and Filtered Tailings, Perth/Online*.
- Fränkle, B., Morsch, P., Nirschl, H., 2021. Regeneration assessments of filter fabrics of filter presses in the mining sector. *Miner. Eng.* 168 (106922).
- Fränkle, B., Morsch, P., Kessler, C., Sok, T., Gleiß, M., Nirschl, H., 2022. Iron ore tailings dewatering: measurement of adhesion and cohesion for filter press operation. *Sustainability* 14 (6), 3424.
- Fränkle, B., Morsch, P., Sok, T., Gleiß, M., Nirschl, H., 2022. Tailings filtration using recessed plate filter presses: improving filter media selection by replicating the abrasive wear of filter media caused by falling filter cake after cake detachment. *Mining* 2 (2), 425–437.
- Fränkle, B., Stockert, M., Sok, T., Gleiß, M., Nirschl, H., 2023. Tailings filtration: water jet spray cleaning of a blinded iron ore filter cloth. *Minerals* 13 (3), 416.
- Ginisty, P., Legoff, B., Olivier, J., Vaxelaire, J., Hervé, T., Paixao, J., 2016. Measurement of adhesion strengths and energy between calcium carbonate cake and filter cloth. *Particle Separation 2016: Advances in Particle Science and Separation: Meeting Tomorrow's Challenges, Oslo*.
- Gomes, R., De Tomi, G., Assis, P., 2016. Iron ore tailings dry stacking in Pau Branco Mine, Brazil. *J. Mater. Res. Technol.* 5 (4), 339–344.
- Grosso, A., Kaswalder, F., Hawkey, A., 2021. Clay-bearing mine tailings analysis and implications in large filter press design. *Proceedings of the 24th International Conference on Paste, Thickened and Filtered Tailings, Thickened and Filtered Tailings, Perth*.
- Gunson, A., Klein, B., Veiga, M., Dunbar, S., 2012. Reducing mine water requirements. *J. Clean. Prod.* 21 (1), 71–82.
- Hammerich, S., Stickland, A., Radel, B., Gleiss, M., Nirschl, H., 2020. Modified shear cell for characterization of the rheological behavior of particulate networks under compression. *Particuology* 51, 1–9.
- Higman, B., Mattox, A., Coil, D., Lester, E., 2019. In: *Trekking, G.T., (Ed.) Mine Tailings. International Council on Mining and Metals (ICMM), 2020. United Nations Environment Programme (UNEP) and Principles of Responsible Investment (PRI)*. In: Oberle, B., Brereton, D., Mihaylova, A. (Eds.) *Global Standard on Tailings Management, Global Tailings Review, London*.
- Islam, K., Murakami, S., 2021. Global-scale impact analysis of mine tailings dam failures: 1915–2020. *Glob. Environ. Chang.* 70 (102361).
- ISO, 2017. ISO 14688-1:2017 - Geotechnical Investigation and Testing — Identification and Classification of Soil — Part 1: Identification and Description. International Organization for Standardization, Geneva.
- Jewell, R.J., Fourie, A.B., 2015. *Paste and Thickened Tailings – A Guide, third ed.* Australian Centre for Geomechanics.
- Kossoff, D., Dubbin, W., Alfredsson, M., Edwards, S., Macklin, M., Hudson-Edwards, K., 2014. Mine tailings dams: characteristics, failure, environmental impacts, and remediation. *Appl. Geochem.* 51, 229–245.
- Lottermoser, B., 2010. *Mine Wastes - Characterization, Treatment and Environmental Impacts, third ed.* Springer-Verlag, Berlin Heidelberg.
- Lottermoser, B., 2017. *Predictive Environmental Indicators in Metal Mining.* Springer International Publishing Switzerland, Cham.
- Ma, X., Fan, Y., Dong, X., Chen, R., Li, H., Sun, D., Yao, S., 2018. Impact of clay minerals on the dewatering of coal slurry: an experimental and molecular-simulation study. *Minerals* 8 (400).
- Micronics, 2020. Micronics' New Mine-XLL™ Filter Cloth Delivers over 10,000 Cycles in Select Mineral Processing Applications. [Online]. Available: <https://www.micronicsinc.com/de/filtration-news/new-mine-xxl-mining-filter-cloth/>. [Accessed 23 June 2023].
- Morrill, J., Chambers, D., Emerman, S., Harkinson, R., Kneen, J., Lapointe, U., Maest, A., Milanez, B., Personius, P., Sampat, P., Turgeon, R., 2022. *Safety First: Guidelines for Responsible Mine Tailings Management v2.0.* Earthworks, MiningWatch Canada, London Mining Network.
- Mortimer, C., Müller, U., 2007. *Chemie, ninth ed.* Georg Thieme Verlag, Stuttgart.
- Nicolaou, I., 1999. *Fortschritte in Theorie und Praxis der Filterkuchenbildung und -entfeuchtung durch Gasdruckdifferenz - Dissertation.* VDI-Verlag, Düsseldorf.
- Metso Outotec, 2022. "Metso:Outotec Pressure Filtration - Larox® FFP & VPA Filters. [Online]. Available: <https://www.metso.com/globalassets/portfolio/larox-ffp-vpa-filters-brochure.pdf?r=3>. [Accessed 26 July 2023].
- Ozcan, O., Ruhland, M., Stahl, W., 2000. Shear strength of mineral filter cakes. *Stud. Surf. Sci. Catal.* 128, 573–585.
- Ozcan, O., Ruhland, M., Stahl, W., 2000. The effect of pressure, particle size and particle shape on the shear strength of very fine mineral filter cakes. *Int. J. Miner. Process.* 59 (2), 185–193.
- Ozcan, O., Gonul, B., Bulutcu, A., Manav, H., 2001. Correlations between the shear strength of mineral filter cakes and particle size and surface tension. *Colloids Surf.* 187–188, 405–413.
- Picullo, L., Storrøsten, E., Liu, Z., Nadim, F., Lacasse, S., 2022. A new look at the statistics of tailings dam failures. *Eng. Geol.* 303 (106657).
- Rahal, K., Wisdom, T., 2020. The impact of thickening on fast filtration of tailings. In: *Proceeding of the Tailings and Mine Waste Conference, Virtual*.
- Roche, C., Thygesen, K., Baker, E., 2017. *Mine Tailings Storage: Safety is No Accident.* United Nations Environment Programme and GRID-Arendal, Nairobi and Arendal.
- Rumpf, H., 1974. *Die Wissenschaft des Agglomerierens.* *Chem. Ing. Tech.* 46 (1), 1–11.
- Schubert, H., 1972. *Untersuchungen zur Ermittlung von Kapillardruck und Zugfestigkeit von feuchten Haufwerken aus körnigen Stoffen - Dissertation.* Universität Karlsruhe, Karlsruhe.
- Schubert, H., 1982. *Kapillarität in Porösen Feststoffsystemen.* Springer, Berlin.
- VDI, 2017. *Mechanical Solid-liquid Separation by Cake Filtration: Mechanical Deliquoring of Incompressible Filter Cakes by Undersaturation Using a Gas Pressure Difference.* Verein Deutscher Ingenieure e.V, Düsseldorf.
- Wang, C., Harbottle, D., Liu, Q., Xu, Z., 2014. Current state of fine mineral tailings treatment: a critical review on theory and practice. *Miner. Eng.* 58, 113–131.
- Weigert, T., 2001. *Haftung von Filterkuchen bei der Fest/Flüssig-Filtration - Dissertation (VDI-Fortschrittsbericht).* VDI-Verlag, Düsseldorf.
- Weigert, T., Ripperger, S., 1997. Effect of filter fabric blinding on cake filtration. *Filtr. Sep.* 507–510.
- Wills, B., Finch, J., 2015. *Wills' Mineral Processing Technology - An Introduction to the Practical Aspects of Ore Treatment and Mineral Recovery, eighth ed.* Elsevier Ltd. (Butterworth-Heinemann), Oxford.
- Wisdom, T., 2019. Maintaining high availability and low operational costs for filtered tailings facilities. In: *Paste 2019: 22nd International Conference on Paste, Thickened and Filtered Tailings, Cape Town*.
- Xiu, Z., Meng, F., Wang, F., Wang, S., Ji, Y., Hou, Q., 2023. Shear behavior and damage evolution of the interface between rough rock and cemented tailings backfill. *Theor. Appl. Fract. Mech.* 125 (103887).